Design of zinc-doped copper ferrite nanostructures using microwave combustion process and its supercapacitive features

M. Selvakumar [a,b], S. Maruthamuthu [b]*, B. Saravanakumar [c], A. Tony Dhiwahar [d]

[a.] *Physics Division, Forensic Sciences department, Chennai - 600 004, Tamil Nadu, India*

[b.] *PSG Institute of Technology and Applied Research Coimbatore - 641 062, Tamil Nadu, India*

[c.] *Dr. Mahalingam College of Engineering and Technology, Pollachi - 642 003, Tamil Nadu, India*

[d.] *Nehru Arts and Science College, Coimbatore - 641 105, Tamil Nadu, India*

Corresponding author: * smaruthamuthu@gmail.com (S. Maruthamuthu)

ABSTRACT

Rapidly increasing demand for electrical energy due to unprecedented growth of electronic gadgets urges the research on developing innovative electrode materials for new age batteries and supercapacitors (SCs). Among various electrode materials for SCs, copper ferrite ($CuFe_2O_4$) is a cost-effective compound to make electrode materials for SC application owing to its expansive multifunctional physical and electrical properties. The nanoparticles of $Cu_xZn_{1-x}Fe_2O_4$ (x=1, 0.9, 0.7 and 0.5) were synthesized *via* a facile and effective microwave combustion route. The effective inclusion of zinc on the surface morphology, size of the nanoparticles, elemental compositions, crystalline nature, and electrochemical properties of $Cu_xZn_{1-x}Fe_2O_4$ (x=1, 0.9, 0.7 and 0.5) were examined by different analytical techniques. The electrochemical investigations reveal the highest specific capacitance of 1250 F g^{-1} for $Cu_{0.9}Zn_{0.1}Fe_2O_4$ which is 61% more than the bare copper ferrite. In addition, supercapacitor device in the form of an asymmetric type has been assembled with an aid of $Cu_{0.9}Zn_{0.1}Fe_2O_4$ electrodes, and an electrochemical performance of the same was investigated using cyclic voltammetry. The assembled device delivered an energy density of 188.75 W h kg^{-1} and a power density of 1249 W kg^{-1}. The simple and cost-effective preparation procedure of $Cu_xZn_{1-x}Fe_2O_4$ with efficient electrochemical features increases the possibility of this material to be a promising electrode for supercapacitor.

Key words: Nanoparticles, ferrites, electrochemical properties, asymmetric supercapacitor

1. Introduction

Man makes his life comfortable using electrical and electronic devices with the help of sensors and remotes, which need electrical energy. Moreover, storage devices used in toys, portable light sources, mobile phones, laptops, hybrid vehicles, satellites and so on demand more energy. Generation of energy from traditional energy resources leads to pollution and induce the climate change. In order to overcome these problems, researchers are working on alternate energy resources and novel energy storage devices [1-3]. Compared to conventional storage devices such as, batteries and capacitors, supercapacitors (SC) store energy with high power density and stability without causing any harm to the ecosystem [4-5]. Hence, SC has become a research hotspot for the development of advanced energy storage devices.

In general, metal oxides and conducting polymers are employed to make a promising class of electrode materials for SC [6]. During the intercalation and de-intercalation process, swell and shrink may take place in the conducting polymers, which results in poor cyclic stability when they act as SC. Hence, researchers have given their attention to metal oxides, especially nanostructured ferrites, for designing electrodes for SC [7]. Ferrites are hybrids of both iron oxides and metal oxides having two different kinds of structures, namely, regular spinel and inverse spinel. The chemical formula for regular spinel ferrite structure is $X^{2+}Fe^{3+}O_4^{2-}$ ($X= Cu^{2+}$, Ca^{2+}, Ni^{2+}, Mg^{2+}, Zn^{2+} or Fe^{2+}). In the spinel ferrite, each divalent metal is enclosed by four O^{2-} ions in a tetrahedral position referred as ‘A’ site and each trivalent is fenced by six O^{2-} ions in an octahedral position referred as ‘B’ site [8].

The extraordinary theoretical capacity, abundance, and non-lethality of copper ferrite (CF) having a spinel structure make it a suitable candidate for fabricating electrode materials for SC. However, owing to poor cyclability, slow kinetics, and poor electrical conductivity, commercialization of copper ferrite-based electrodes has been limited [9]. In order to overcome these problems, CF is doped with Zn ions in the place of copper in order to make promising electrodes for supercapacitor applications. The crystal structure of copper ferrites changes from normal to inverted spinel by doping copper ferrites with Zn ions. Further, the position and composition of the parent material can be altered to enhance the structural to some extent, electrical, optical, and magnetic properties. Especially, metal ferrites doped with Zn^{2+} are being mainly used in numerous devices namely gas-sensing devices, spintronic devices and massive storage devices and so on.

V. Sharma et al. designed hierarchical porous super-architecture t-$CuFe_2O_4$ solid-state asymmetric SCs and increased the specific capacity three-fold by inserting a redox additive into the electrolyte [10]. Mubasher and M. Mumtaz et al. employed chemical co-precipitation to synthesize pure CF nanoparticles and ultra-sonication method for the formation of CF/multiwall carbon nanotube [11]. E. Samuel et al. reported beehive-like $NiFe_2O_4$ ultrathin nanosheets for constructing high-energy-density SC electrodes to improve capacitance and electrochemical performance [12]. Bin Li et al. synthesized well-dispersed crystalline spinel type complex metal oxide like $NiFe_2O_4$ and $CuFe_2O_4$ nanoparticles supported on mesoporous silica to increase specific capacitance [13]. A. Manikandan et al. prepared pure zinc ferrite and copper-doped zinc ferrite $Zn_{1-x}Cu_xFe_2O_4$ nanoparticles by microwave combustion method and analyzed the magnetic properties [14]. Nanocrystals of unalloyed and Mg-incorporated $ZnFe_2O_4$ ($Zn_{1-x}Mg_xFe_2O_4$ in which the value of x runs from 0.0 to 0.8 in the step of 0.1) were synthesized by microwave combustion with urea as fuel. Doping Mg^{2+} ions was found to increase the ferromagnetic behavior of the material (up to x = 0.5), which reshaped the hysteresis loop [15]. A. Tony Dhiwahar et al. synthesized $Cu_{1-x}Zn_xFe_2O_4$ (x = 0.1, 0.2, 0.3, 0.4, and 0.5) nanoparticles *via* microwave-assisted combustion, which exhibited a soft magnetic nature [8]. Thanh et al. selected spray co-precipitation route to synthase nickel-substituted copper ferrites ($Cu_{1-x}Ni_xFe_2O_4$, the value of x changes as 0.0, 0.3, 0.5, 0.7, and 1) and confirmed the altered magnetic properties caused by Ni doping on it. The increasing nickel content was the key factor disturbing the saturation magnetization property of the specimen [16]. Wang Zhang et al. prepared multifunctional $CuFe_2O_4$/Graphene that showed extraordinary supercapacitor performance [17]. S. Martinez-Vargas, et al. found that an increase in cobalt concentration in the cobalt ferrite nanoparticles increases the size of the nanoparticles, their magnetic coercivity and electrical conductivity. Furthermore, the presence of cobalt ferrite nanoparticles in the supercapacitor provided more surface area for ion storage [18]. In the present study, we investigate the enhancement of super capacitive behavior due to the inclusion of zinc atom in place of copper atom in copper ferrite nanoparticles at three different wt. percentages of 0.1, 0.3 and 0.5. Facile microwave combustion process was employed to synthesize the nanoparticles of $Cu_xZn_{1-x}Fe_2O_4$, where x=1, 0.9, 0.7, and 0.5. The present work reports the chemical compositions, functional groups, surface features and crystalline nature of the synthesized copper ferrite with and without the incorporation of Zn atoms and charge storage properties of bare copper ferrite and Zn-fused copper ferrite electrodes using a three-electrode cell with the aid of cyclic voltammetry (CV). The asymmetric supercapacitor device was made up of Zn-doped copper ferrite electrode and an activated carbon (AC) electrode with high surface area.

2. Experimental

2.1 Synthesis of CF and ZCF samples

The nanoparticles of $Cu_xZn_{1-x}Fe_2O_4$ (where x=1, 0.9, 0.7, and 0.5) have been prepared by a simple microwave combustion technique using analytical grade all with 98% purity of zinc nitrate ($Zn(NO_3)_2.6H_2O$), copper nitrate ($Cu(NO_3)_2.3H_2O$) ferric nitrate ($Fe(NO_3)_3.9H_2O$, and L-arginine ($C_6H_{14}N_4O_2$) acquired from Merck dealers in India. Concisely, 0.808 g of $Fe(NO_3)_3.9H_2O$, 0.0297 g of $Zn(NO_3)_2.6H_2O$, 0.2174 g of $Cu(NO_3)_2.3H_2O$, and 0.2664 g of $C_6H_{14}N_4O_2$ as fuel have been dissolved in 50 mL of water (double-distilled) by keeping the fractional ratio of fuel to oxidizer as unity [fuel (U)/oxidizer (N) =1] in order to release the maximum energy for the reaction [19]. The mixed solution was kept on magnetic stirring device, stirred pretty slowly for an hour and carefully transported to a 150 mL crucible made up of silica. For the combustion process, the stirred solution was placed in a home adapted 800 W with recurrence frequency of 2.54 GHz microwave oven device (model no. CE1041DFB/XTL) with a reaction time of ten minutes. The samples have been taken out from the microwave oven after the combustion process and maintained at the temperature of 500 □ for 2 hours, on which nanoparticles of $Cu_{0.9}Zn_{0.1}Fe_2O_4$ (ZCF1) were obtained. Following the above general procedure, the prepared nanoparticles of compositions $Cu_{0.7}Zn_{0.3}Fe_2O_4$ and $Cu_{0.5}Zn_{0.5}Fe_2O_4$ are named as ZCF3 and ZCF5, respectively. Same procedure was implemented without using Zn source to prepare bare copper ferrite (CF) nanoparticles.

2.2 Structural characterization of CF and ZCF nanoparticles

The XRD patterns of bare CF and ZCF samples were acquired from RIGAKU X-ray diffractometer (powder) with Cu Kα (λ = 1.5418 Å) radiation with 2θ (diffracted angle) ranging from 20 to 80° and the Fourier Transform Infra-Red (FT-IR) absorption spectra of CF and ZCF samples were obtained *via* Nicolet iS10 spectrometer in the wavenumber region between 500 cm^{-1} and 4000 cm^{-1}. The surface morphological examinations were carried out at 500 nm scale with the help of a High-resolution Scanning Electron Microscope (SEM) (model no. JEOL 6360) system attached with energy dispersive X-ray analysis (EDX) to identify the elemental compositions of CF and ZCFs.

2.3 Electrochemical analysis

The electrochemical measurements of CF and ZCFs were studied at room temperature using a USA make electrochemical plant (CH Instruments Inc., Model no. CHI 660C,) employing a three-electrode setup. For electrochemical measurements, a conventional electrochemical cell was set up with prepared CF or ZCFs samples as working electrode, an

Ag/AgCl as reference electrode, and a platinum wire as counter electrode. The working electrode was made by mixing 5 wt % of binding material such as polytetrafluoroethylene (PTFE), 10 wt % of carbon black (Super-P), 85 wt % of prepared sample, and ethanol as solvent. This slurry has firmly been coated on a cleaned in advanced nickel foam of geometrical area of 1 cm^2 and dried at 60 □ for 2 hrs. Nickel foam was cleaned using 37 wt % of HCl to eradicate the undesirable materials present on the surface prior to coating the active material. It was also washed with ethanol plus double distilled water. Potassium hydroxide (2 M) solution was used as the electrolyte. The asymmetric supercapacitor device was fabricated using ZCF and activated carbon (AC) with specific area of 1100 m^2/g obtained from Sigma-Aldrich as positive and negative electrodes respectively, 2 M KOH as the electrolyte and polypropylene as the separator in which the electrochemical features of supercapacitive were calculated using the active electrode mass of 0.8 mg. The following equations were used to assess the electrochemical features of Zn-doped copper ferrite asymmetric supercapacitor device.

Specific capacitance $C_s = \frac{I * dt}{m * dv}$,----------(1)

where C_s, *I/m*, *dt* (s), and *dv* (V) are the specific capacitance, current density in terms of A g^{-1}, discharge time measured in second and potential window in terms of voltage, respectively.

Energy density $E = \frac{1}{2 * 3.6} C_S * (\Delta V)^2$----------(2)

Power density $P = \frac{E}{t} * 3600$,----------(3)

where *E* (W h kg^{-1}), *P*(W kg^{-1}) and t (s) represent energy density, power density and time of discharge, respectively.

3. Results and Discussion

3.1 Structural and morphological analysis

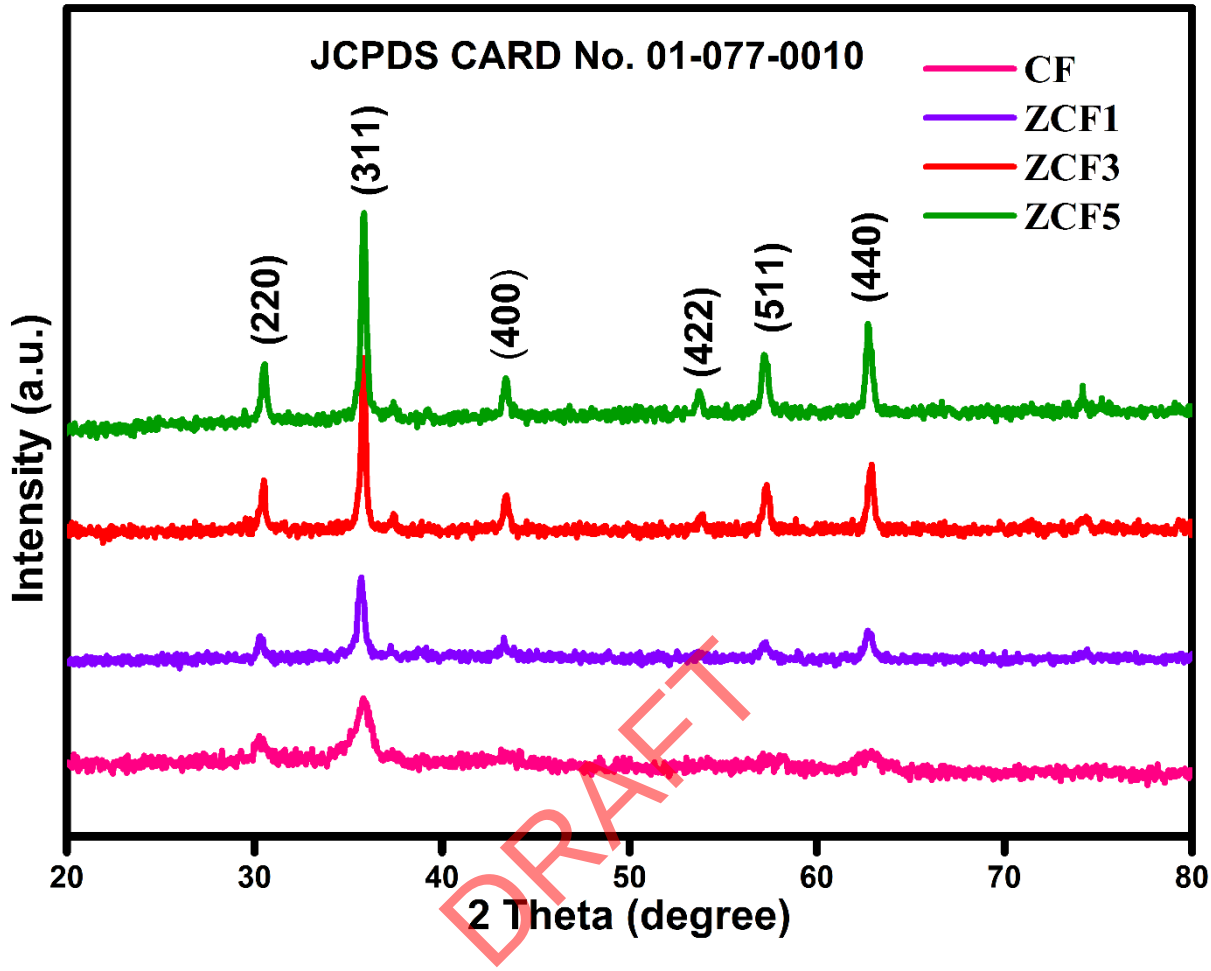

Fig. 1. XRD spectra of bare CF and ZCF samples

Fig. 1 illustrate the XRD profiles of CF, ZCF1, ZCF3, and ZCF5. The predominant peaks observed at 30.30°, 35.70°, 43.30°, 53.67°, 57.27°, and 62.72° are linked to diffraction from (220), (311), (400), (422), (511), and (440) planes of the cubic crystal structure with Fd-3m space group. These values are in accordance with the JCPDS card no. 01-077-0010 [17]. The predominant peaks from (311) planes observed at 35.789°, 35.683°, 35.811° and 35.824° for CF, ZCF1, ZCF3 and ZCF5, respectively. The peak shift is ± 0.1°. The average size of the above nanocrystallite is estimated from full width half maximum (Debye Scherrer formula, Lorentz fit method) choosing the (311) plane. The values were found to be 19.3, 22.52, 34.02, and 29.82 nm for CF, ZCF1, ZCF3, and ZCF5, respectively. Smaller size could assist diffusion of ions in the electrolyte which results in higher capacitance [20].

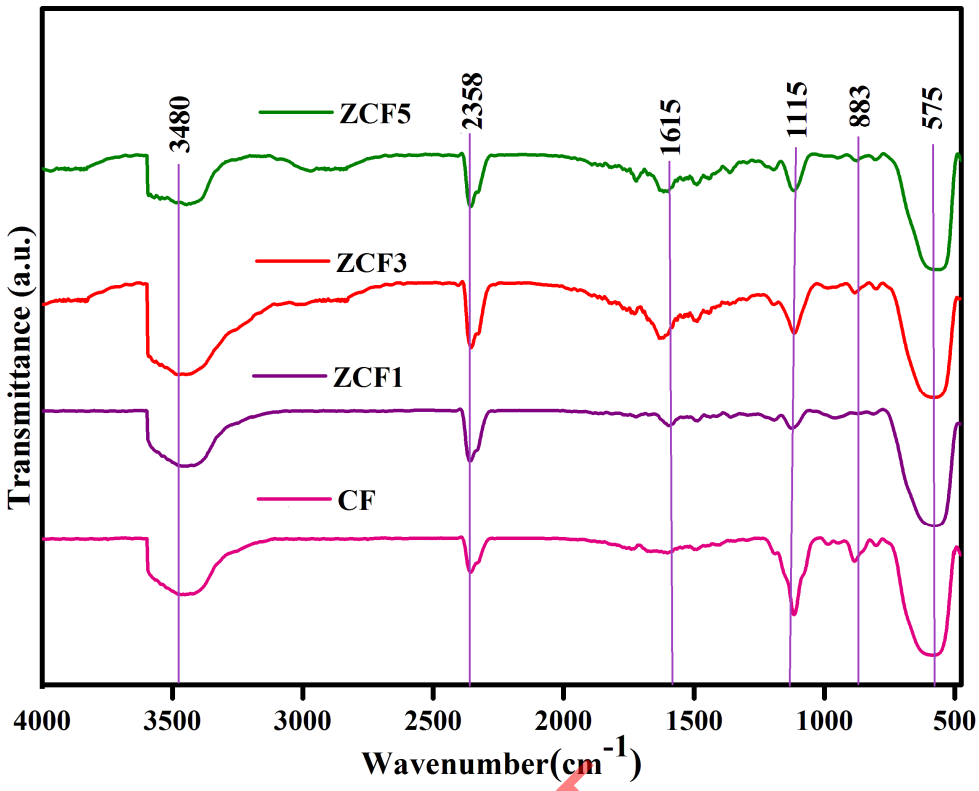

Fig. 2 – FT-IR spectra of bare CF and ZCF samples

With the aim of check the functional groups existing in CF and ZCF composites, FT-IR was performed. Fig. 2 illustrates the FT-IR spectra of bare CF, ZCF1, ZCF3, and ZCF5 scanned from 4000 to 500 cm^{-1} at ambient temperature. In the spectra of all the materials, a band is observed at 575 cm^{-1} owing to inherent elongating vibrations of Fe^{3+}–O^{2-} in the tetrahedral sites. A band at 3480 cm^{-1} was caused by the residual water molecule in the sample [21]. In addition, the peak at 1615 cm^{-1} results from the chemisorbed species. Furthermore, the band at 2358 cm^{-1}denotes the physisorbed CO_2 species [22].

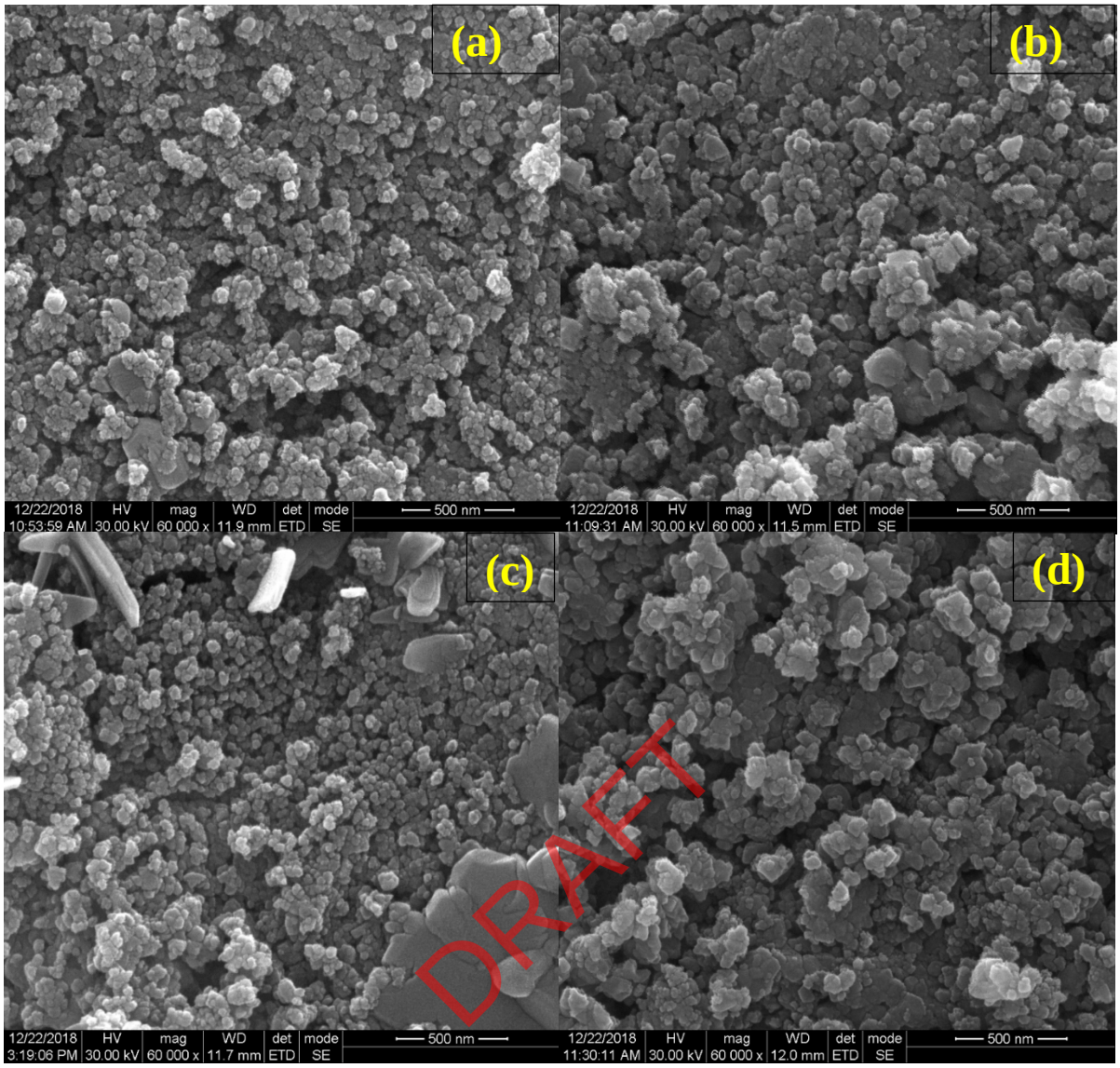

Fig. 3 – SEM images of (a) bare CF (b) ZCF1, (c) ZCF3 and (d) ZCF5 at 500 nm scale

The surface morphology of a nanomaterial significantly impacts its selection for making electrode for SCs. Hence, HR-SEM examination was executed to analyze the surface morphology of $Cu_xZn_{1-x}Fe_2O_4$ (x=1, 0.9, 0.7, and 0.5) nanoparticles. The SEM images presented in Fig. 3 reveal that the synthesized nanoparticles are homogeneous and agglomerated. The average particle size of CF, ZCF1, ZCF3, and ZCF5 are in the order of nanometer which is in good agreement with estimated particle size from x-ray diffraction pattern. Among all the nanoparticle systems, ZCF1 showed uniformly distributed and well-defined spherical crystallites with a uniform texture making it a suitable candidate for fabricating electrodes for SC.

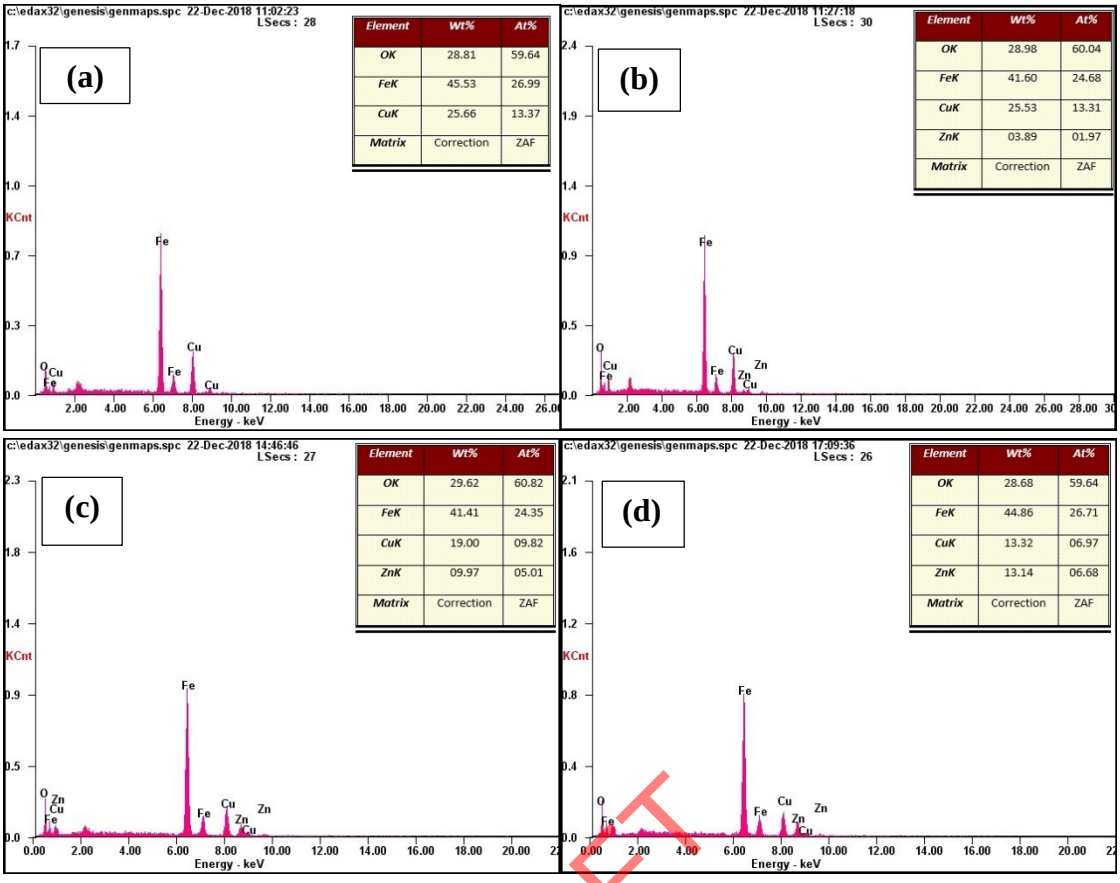

Fig. 4 – EDX spectra of (a) bare CF (b) ZCF1, (c) ZCF3 and (d) ZCF5

Energy dispersive X-ray analysis was performed on CF and ZCF samples in order to evaluate the percentage of elemental composition present in the samples and its spectra were shown in Fig. 4. The results confirm the successful incorporation of Zn in copper ferrite in place of copper and the presence of O, Fe, Cu and Zn in the samples. The compositions of Zn and Cu obtained from EDX profile of CF and ZCF agree well with the required quantity of Zn and Cu on the basis of stoichiometric calculations and the data are listed in Table 1.

Table 1. The measured and anticipated atomic and weight percentage of elements in CF and ZCFs

S. No.	Composites	Percentage	OK	FeK	CuK	ZnK	Total
1	CF	Wt. % (M)	28.81	45.53	25.66	00.00	100.00
		Wt. % (A)	26.74	46.69	26.57	00.00	100.00
		At. % (M)	59.64	26.99	13.37	00.00	100.00
		At. % (A)	57.14	28.57	14.29	00.00	100.00
2	ZCF1	Wt. % (M)	28.98	41.60	25.53	03.89	100.00
		Wt. % (A)	26.71	46.66	23.89	02.74	100.00
		At. % (M)	60.04	24.68	13.31	01.97	100.00
		At. % (A)	57.14	28.57	12.86	01.43	100.00
3	ZCF3	Wt. % (M)	29.62	41.41	19.00	09.97	100.00
		Wt. % (A)	26.68	46.59	18.54	08.19	100.00
		At. % (M)	60.82	24.35	09.82	05.01	100.00
		At. % (A)	57.15	28.57	09.99	04.29	100.00
4	ZCF5	Wt. % (M)	28.68	44.86	13.32	13.14	100.00
		Wt. % (A)	26.70	46.50	13.20	13.60	100.00
		At. % (M)	59.64	26.71	06.97	06.68	100.00
		At. % (A)	57.15	28.57	07.14	07.14	100.00

3.2 *Electrochemical Analysis of CF and ZCFs electrodes*

The electrochemical performances of CF and ZCFs electrodes were investigated using CV and galvanostatic charge-discharge (GCD) in a conventional three-electrode arrangement in the potential window between 0 and 0.5 mV s^{-1} in 2 M KOH aqueous electrolyte and the comparison of electrochemical behaviour of CF and its composites is given in Table 2. Fig. 5 (a) depicts the CV graphs of CF, ZCF1, ZCF3, and ZCF5 electrode materials at the rate of sweep voltage of 5 mV s^{-1}. These CV graphs show the presence of well-defined oxidation and reduction peaks. During the anodic current, electrode is oxidized by emitting the electrons, unbalancing charges leaving the material, corresponding to the anodic peaks at a potential of 0.33 and 0.4 V, since copper exists two oxidation states namely +1 and +2. While the cathodic current, the cathodic peaks ($Cu^{2+/+}$ - Cu^{0}) are seen at around 0.27 and 0.19 V for all scan rate. These peaks firmly indicate the influence of redox reactions during ion intercalation and deintercalation process. Further, it is evident that the closed loop area of CV curve of ZCF1 was reasonably

greater than those of ZCF5, ZCF3, and CF. This indicated that ZCF1 have enhanced the electrochemical activity and specific capacitance attributable to the electrochemically active Zn^{2+} ions that reduce the internal resistance in the samples.

The GCD measurements were performed to analyze the charge storage capacity of $Cu_xZn_{1-x}Fe_2O_4$ (x=1, 0.9, 0.7, and 0.5) samples. The GCD graphs of CF, ZCF1, ZCF3, and ZCF5 electrodes in the potential range from 0 to 0.4 V at a current density of 1 A g^{-1} have been depicted in Fig 5 (b). The non-linear GCD graphs emphasized the impact of redox responses over the EDLC behavior of the Zn-un doped and doped samples.

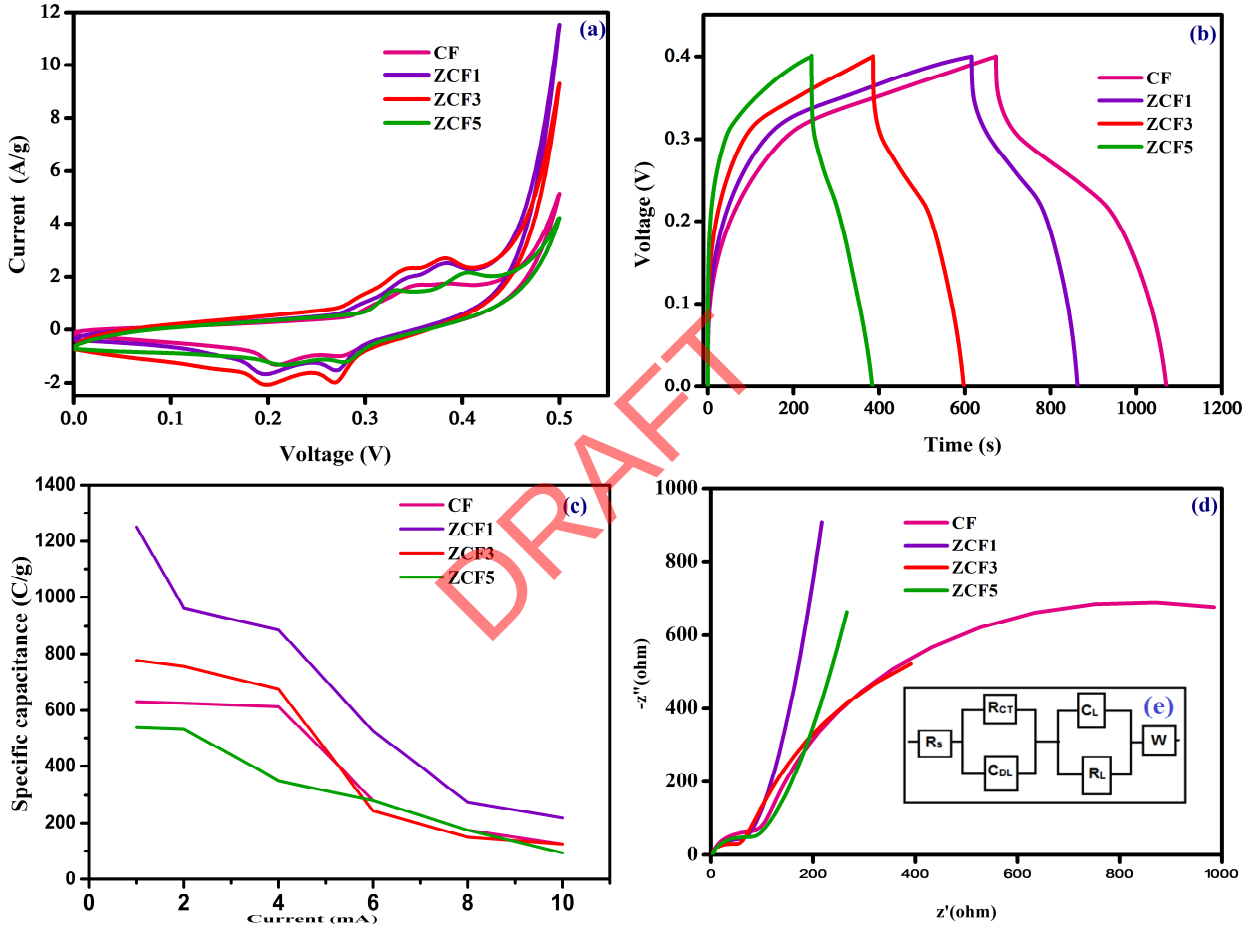

Fig. 5 (a) CV graph profiles of CF and ZCF electrodes at a voltage scan rate of 5 mV s^{-1}, (b) GCD graph profiles of CF and ZCF electrodes at a constant current rate of 1 A g^{-1}, (c) Deviation of capacitance at different current densities, (d) Nyquist plot for CF and ZCF electrodes (inset (e) modified Randles circuit model).

Fig. 5 (c) shows the variation of specific capacitance of CF and ZCFs electrode with respect to current in the step of 1 A g^{-1}. Using equation (1), the specific capacitance has been estimated to be 538, 778, 1250 and 620 F g^{-1} for ZCF5, ZCF3, ZCF1, and CF, respectively. Due to bimetallic effect of Cu-Zn, electrolyte ions in the electrolyte have adequate time to reach the active sites of the electrodes made up of CF and ZCFs at lower current zone resulting in larger

specific capacitance values in addition to that the remarkable improvement in the electrochemical performance is attributed to the small size of ZCF1[23]. These results are comparable with the values reported by other research groups. B. Mordina et al. achieved the maximum specific capacity value of 925 F g^{-1} at 1 A g^{-1} current density with $NiFe_2O_4$ nanoparticle-derived positive electrode, activated carbon negative electrode and Ni-foam current collector using 6 M KOH solution [24]. U. Wongpratat et al. came out with a specific capacitance values of 259.89 F g^{-1} with $MgFe_2O_4$ as the working electrode, a platinum wire as the counter electrode and an Ag/AgCl as the reference electrode in 6 M KOH [25]. V. Vignesh et al. obtained a maximum specific capacitance of 173 F g^{-1} at 1 A g^{-1} for $MnFe_2O_4$ electrode in 3.5 M KOH [26]. Ankur Soam et al. reported a high specific capacitance with nickel ferrite/graphene in 1 M Na_2SO_4 electrolyte [27] B. Bhujun et al. reported a specific capacitance value of 548 F g^{-1} at a scan rate of 100 mV/sec scan rate for $Al_{0.2}Cu_{0.4}Co_{0.4}Fe_2O_4$ nanocomposite in 1 M KOH aqueous electrolyte solution [28]. A specific capacitance of 747.64 F/gat 1 mA/g has been reported for ternary polyaniline-acetylene black-cobalt ferrite composite with 1 M KOH solution by T. Das et al. [29]. In another work, cobalt-substituted zinc-ferrite nanoparticles showed a specific capacitance of 377.81 F g^{-1} when used as an electrode in a pseudo-capacitor in 1 M aqueous NaOH electrolyte [30].

The capacitive behavior is primarily persuaded by current density. The charge-discharge profiles of ZCFs and CF electrodes in a 2 M KOH electrolyte at various current densities (1 to 10 A g^{-1}) are shown in Fig. 5 (c). For all the electrodes, the highest specific capacitance was 1250 F g^{-1} for ZCF1 at the lowest current density of 2 A g^{-1}, which diminished further for higher current densities. It is because of part of voltage is utilized to overcome the IR drop and the remaining voltage is employed to charge the supercapacitor made up of CF/ZCF nanoparticles. Hence, the resultant voltage (ΔV) window will be shrunk. The IR drop is due to summative resistances offered by electrodes of CF/ZCFs, electrolyte (2 M KOH) and contact resistances of three-electrode cell configuration. The IR drop of CF, ZCF1, ZCF3, and ZCF5 are 3.05, 0.84, 1.49, and 2.4 Ω, respectively. At higher current density, there is a loss of energy due to IR drop which will be significant after aging i.e., number of cycles including both charging and discharging.

In order to study the collective behaviour of resistive and capacitive features of any SC electrode materials, electrochemical impedance spectra (EIS) analysis is a better diagnostic procedure. The EIS studies of CF and ZCFs electrodes were executed, and the Nyquist graph is illustrated in Fig 5 (d) and modified Randles electronic circuit model is presented in Fig 5 (e) as inset in Fig 5 (d). In the modified Randles circuit, R_{CT}, D_{DL}, C_L, and W represent resistance due

to charge transfer, double layer capacitance, mass capacitance, and Warburg element, respectively. Intercept on the z' axis (X-axis) made by a semicircle which represents charge transfer resistance (R_{CT}) from ion interfacing on the electrode in Nyquist plot. From the graph, the estimated R_{CT} information of CF, ZCF1, ZCF3, and ZCF5 electrodes are 86, 51, 54, and 82 Ω, respectively. The R_{CT} values of CF and ZCFs electrode indicates the low concentrated Zn-doped samples such as ZCF1 and ZCF3 display the least charge transfer resistance compared to that of bare CF electrode. This poorer R_{CT} could be the predominent view for greater capacitance and superior electrochemical behaviour of ZCF1 as well. This least R_{CT} will enable enhanced charging and discharging phenomena of electrodes through ion exchange or ion transportation between electrode and electrolyte boundary at higher current densities of ZCF1 supercapacitor. [31]

Table. 2. – Comparison of electrochemical behaviour of CF and its composites

S.No.	Composites	Specific capacitance	R_{CT}	IR drop	Rank
Unit		$F\ g^{-1}$	Ω	Ω	
1	CF	620	86	3.05	3
2	ZCF1	1250	51	0.84	1
3	ZCF3	778	54	1.49	2
4	ZCF5	538	82	2.4	4

3.3 Asymmetric supercapacitor behavior of zinc-doped copper ferrite supercapacitor device

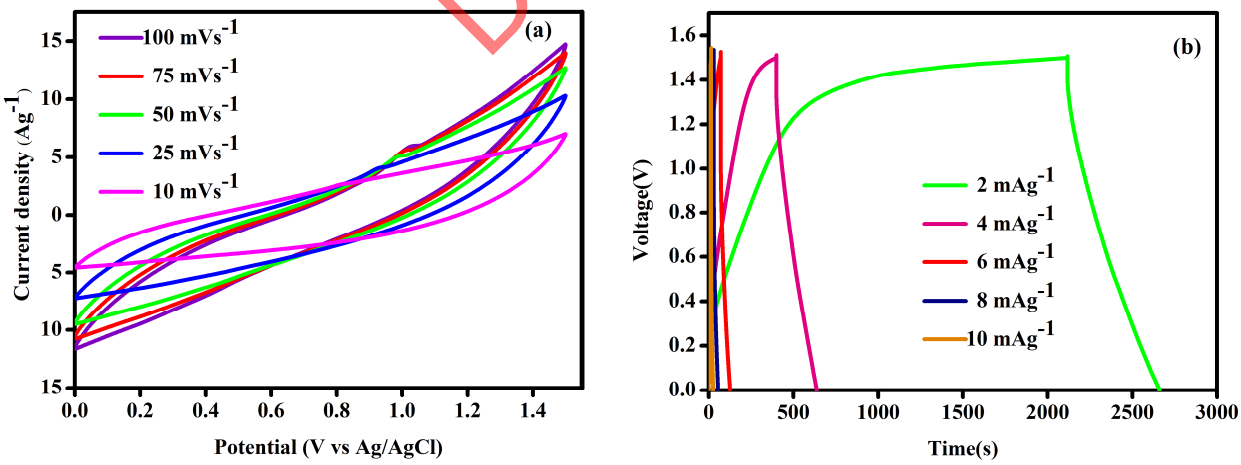

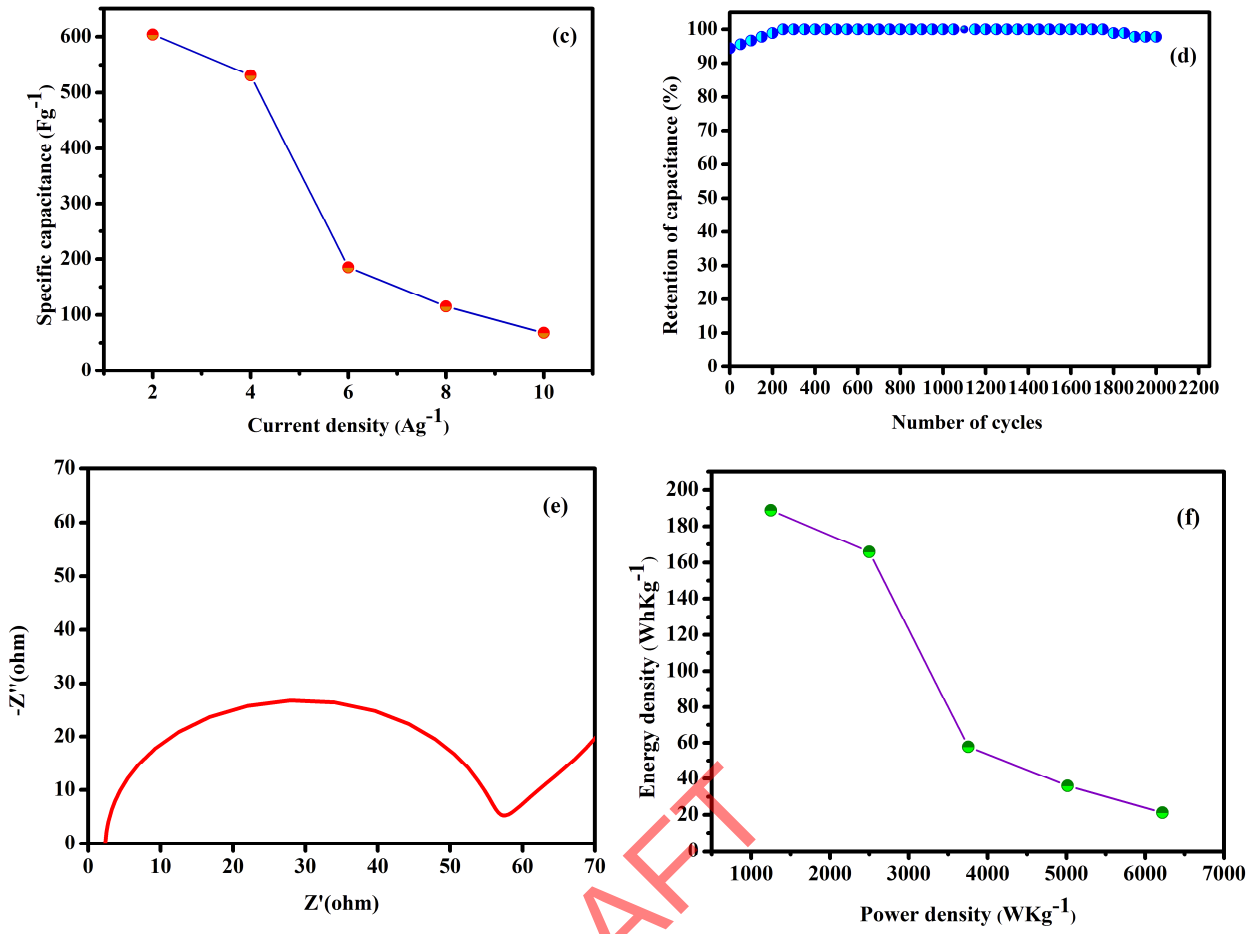

Fig. 6 (a) CV profiles of ZCF1//AC device at various voltages, (b) GCD curves of ZCF1//AC at various current densities, (c) Variation of specific capacitance with current density of ZCF1//AC device, (d) Cyclic stability plot for ZCF1//AC device, (e) Nyquist plot for ZCF1//AC device and (f) Ragone plot of ZCF1//AC device

In general, electrochemical analysis with a twin electrode device is more consistent to examine the adaptableness of the synthesized sample for commercial applications. Using ZCF1 and high surface AC, a two-electrode configuration with an asymmetric SC device was fabricated on an electrochemical workstation. Polypropylene in the form of sheet has been used as divider with 2 M KOH electrolyte, ZCF1//AC can be considered as two capacitors connected in series and the reciprocal of its actual capacitance (Ceff) is equal to the sum up of the one over the capacitances of both electrodes. Electrochemical performance of ZCF1//AC asymmetric type supercapacitor is given in Table. 3. Fig. 6 (a) displays the CV profiles of ZCF1//AC device (asymmetric type) at various voltage scan rates between 10 and 100 mV s^{-1} in the voltage (potential) frame between 0 V and 1.4 V. From the graph profile, it could be observed that a kind of pseudo-rectangular contour was found to be retained at all sweep rates, which indicates the improved repeatability, reversibility and good capacitive behaviour of the ZCF1//AC device. The GCD measurements were carried out for this device at different current densities from 2 to 10 A

g^{-1} with a step of 2 A g^{-1} and they are presented in Fig. 6 (b). In addition, the specific capacity of the asymmetric supercapacitor device of ZCF1//AC was measured using the area of the discharge curves and the maximum specific capacitance was measured to be 604 F g^{-1} for ZCF1//AC device at 2 A g^{-1} since the estimated specific capacitance values of the device are 604, 531, 185, 115, 68 at 2, 4, 6, 8, 10 A g^{-1} respectively which is depicted in Fig. 6(c). The cyclic stability investigation for this device is depicted in Fig. 6 (d). The cyclic stability of the SC was found to be 98 % till 2000 cycles at the current rate of 10 A g^{-1} that governs its overall performance. Between CV and GCD to assess the capacitance value of a supercapacitor, GCD is preferable since in this technique, the quantum of energy stored is quantified with the runtime of the experiment, whereas in CV, the analysis time is governed by the rate at which the scanning takes place and the width of the potential window. The mass ratio $(m_+/m_-) = (C_-V_-)/(C_+V_+)$ governs the mass to be balanced during the charging-discharging process, where C_+ and C_- are the specific capacitances (in F/g) measured at the same scan rate, m_-, and m_+ are the mass (mg) of the fabricated electrode made of AC (cathode) and ZCF1 (anode) respectively, C is the capacitance of the ZCF (F g^{-1}) and V is the potential window (V) between ZCF and AC electrodes. The optimised mass ratio of ZCF1 and AC are 0.8 mg and 0.4 mg respectively. Hence, the aggregate mass of the electrode system would be 1.2 milligram using the above equation, m_+ =2 mg in order to balance the mass in the fabricated supercapacitor device. It is well known that beyond 1V, electrolyte made up of aqueous KOH is a high degree of susceptible to the oxygen evolution reaction. Thus, the potential window is limited between 0 and 1 V for ZCF1-based SC using 2 M KOH aqueous electrolyte.

Table. 3. Electrochemical performance of ZCF1//AC asymmetric type supercapacitor

S.No.	Current density	Specific capacitance	Energy density	Power density
Unit	A g^{-1}	F g^{-1}	W h kg^{-1}	W kg^{-1}
1	2	604	188.8	1249
2	4	531	165.9	2499
3	6	185	57.8	3756
4	8	115	35.94	5014
5	10	68	21.25	6219

The Nyquist plot for ZCF1//AC asymmetric device is displaced in Fig. 6 (e). The R_{CT} value of this device is 55 Ω, which is slightly greater than the R_{CT} values estimated using three-electrode cell arrangement, it is because of addition of activated carbon, which imparts a minor resistance. The energy and power density of zinc doped copper ferrite device were calculated

using equations (2) and (3), respectively. The calculated values of energy and power densities of ZCF 1 are 188.75 W h kg^{-1} and 1249 W kg^{-1} based on GCD investigation and the fluctuations of energy density with respect to power density is depicted in Fig. 6 (f) as Ragone plot. The energy and power density of ZCF1 are higher than those reported for similar supercapacitors. M. Khairy et al. reported as-synthesized $CuFe_2O_4$ as an outstanding electrode candidate for SC application with a maximum specific capacitance of 145 F g^{-1}, energy density of 18.9 W h kg^{-1} and power density of 486 W kg^{-1} at the current density of 1 A g^{-1} [32]. J. Song et al. reported flexible rGO/$CoFe_2O_4$/PEDOT: PSS paper electrode with a specific energy of 25.9 W h kg^{-1} at 1 mA g^{-1} and 135.3 W kg^{-1} as power density [33]. Tapas Das et al. reported polyaniline-acetylene black-$CuFe_2O_4$ electrode, which exhibited an energy density and a power density of 38.81 W h kg^{-1} and 125 W kg^{-1}, respectively at current density of 1 mA [29]. Amirmohammad Khosravi Ghasemi et al. fabricated PANI/GO/$CuFe_2O_4$ electrode for supercapacitor and reported an energy density of 49.72 W h Kg^{-1} and a power density of 923 W kg^{-1} at 1 A g^{-1} [34]. The $CuFe_2O_4$/rGO electrode reported by B.C.J. Mary et al. exhibited 98 % of capacity retention with a specific energy of 18.3 W h k g^{-1} and a specific power of 455 W kg^{-1} [35]. The $CuFe_2O_4$ nanocomposites prepared by solvothermal synthesis showed a maximum capacitance value of 334 F g^{-1} in 1 M KOH at 6 A g^{-1} [36]. It can be decided that ZCF electrodes could be a potential candidate for high-performance SC devices from the above investigation.

4. Conclusions

Pure nanocrystalline Cu-Zn ferrite nanoparticles have been synthesized by combustion, a reliable and facile process, for supercapacitor application. The electrochemical behavior of Zn-doped copper ferrite nanoparticles $Cu_xZn1_{-x}Fe_2O_4$ (x=1, 0.9, 0.7, and 0.5) were analyzed. The presence of Zn has improved the electrochemical properties. Among the different concentration of Zn in copper ferrite, $Cu_{0.9}Zn_{0.1}Fe_2O_4$ exhibited the maximum specific capacitance of 1250 F g^{-1} in the 2 M KOH electrolyte. Our studies reveal that the performance of ZCF1 ($Cu_{0.9}Zn_{0.1}Fe_2O_4$) electrode in 2 M KOH electrolyte is superior than the other Zn-doped copper ferrite samples. The ZCF//AC supercapacitor delivered the maximum energy (188.75 W h kg^{-1}) and power density (1249 W kg^{-1}) at a current density of 2 A g^{-1}.

Conflict of interest

The authors declare that they have no conflicts of interest

Ethical approval

I am the corresponding author and I declare that the manuscript should not be submitted to more than one journal for simultaneous consideration. The authors agree to publish the manuscript in the Journal of Materials Science: Materials in Electronics

Financial Competitive

The authors declare no competing financial interest.

Research Data Policy and Data Availability Statements

The data generated during the current study are available from the corresponding author on reasonable request.

Author Contribution

All author contribute equally to this work

M. Selvakumar contributes to conceptualization, methodology and synthesis of Nanoparticles

S. Maruthamuthu contributes to coin the problem and frame of workflow, formal analysis data collection

B. Saravanakumar contributes to interpretation of data and reviewing of workflow

A. Tony Dhiwahar contributes to draft writing and reviewing and editing the manuscript

5. References

[1] Xiai Zhang, Haitao Liu, Chen Liang, Fujun Ren, Jinyuan Zhao, Tong Wang, Rui Zhong, Deyi Zhanga and Hao Zhub, "Preparation of uniform and highly dispersed magnetic copper ferrite submicron sized particles regulated by short-chain surfactant with catechol structure: Dual-functional materials for supercapacitor and dye degradation," *Journal of Electroanalytical Chemistry*, vol. 870, p. 114199, 2020.

[2] M.Inagaki, H.Konno and O.Tanaike, "Carbon materials for electrochemical capacitors," *Journal of Power Sources*, vol. 195 pp. 7880–7903, 2010.

[3] R. Khan, M. Habib, M.A. Gondal, A. Khalil, Z.U. Rehman, Z.Muhammad, Y.A. Haleem, C. Wang, C.Q. Wu and L. Song, "Facile synthesis of $CuFe_2O_4$-Fe_2O_3 composite for high

performance supercapacitor electrode applications," *Materials research express*, vol.4 p. 105501, 2017.

[4] Y. Wu, G. Gao, H. Yang, W. Bi, X. Liang, Y. Zhang, G. Zhang and G. Wu, "Controlled synthesis of V2O5/MWCNTs core/shell hybrid aerogels through a mixed growth and self–assembly methodology for supercapacitors with high capacitance and ultralong cycle life", *Journal of Materials Chemistry A*, 3, p.15692, 2015.

[5] Wenchao Bi, Guohua Gao, Yingjie Wu, Huiyu Yang, Jichao Wang, Yuerou Zhang, Xing Liang, Yindan Liu and Guangming Wu, "Novel three-dimensional island-chain structured V2O5/graphene/MWCNT hybrid aerogels for supercapacitors with ultralong cycle life", RSC Advances, 7, pp. 7179–7187, 2017.

[6] Lijun Fu , Qunting Qu , Rudolf Holze, Veniamin V. Kondratiev and Yuping Wu, "Composites of metal oxides and intrinsically conducting polymers as supercapacitor electrode materials: The best of both worlds," *Journal of Materials Chemistry A*, vol. **7**, pp. 14937-14970, 2019.

[7] Ran Tao, Jianguo Zhu, Yuefei Zhang, Wei-Li Song, Haosen Chen and Daining Fang, "Quantifying the 2D anisotropic displacement and strain fields in graphite-based electrode via in sity scanning electron microscopy and digital image correlation," *Extreme Mechanics Letters*, vol. 35, p. 100635, 2020.

[8] A. Tony Dhiwahar, M. Sundararajan, P. Sakthivel, Chandra Sekhar Dash and S. Yuvaraj, "Microwave-assisted combustion synthesis of pure and zinc-doped copper ferrite nanoparticles: Structural, morphological, optical, vibrational, and magnetic behavior," *Journal of Physics and Chemistry of Solids*, vol. 138, p. 109257, 2020.

[9], E. Prince and R.G. treating, "The structure of tetragonal copper ferrite", Acta crystallographia, vol. 9 pp. 1025-1028, 1956.

[10] Vikas Sharmaa, Uday Narayan Pana, Thangjam Ibomcha Singha, Amit Kumar Dasa, Nam Hoon Kima, Joong Hee Leea, "Pragmatically designed tetragonal copper ferrite super-architectures as advanced multifunctional electrodes for solid-state supercapacitors and overall water splitting," *Chemical Engineering Journal*, vol. 415 p. 127779, 2021.

[11] Mubasher, M. Mumtaz, "Nanocomposites of multi-walled carbon nanotubes/cobalt ferrite Nanoparticles: Synthesis, structural, dielectric and impedance spectroscopy," *Journal of Alloys and Compounds*, vol. 866, p. 158750, 2021.

[12] Edmund Samuel, Ali Aldalbahi, Mohamed El-Newehy, Hany El-Hamshary, Sam S. Yoon, "Nickel ferrite beehive-like nanosheets for binder-free and highenergy-storage supercapacitor electrode", *Journal of Alloys and Compounds,* vol. 852, p. 156929, 2021.

[13] Bin Li, Min Li, Chaohua Yao, Yifeng Shi, Danru Ye, Jing Wu and Dongyuan Zhao, "A facile strategy for the preparation of well-dispersed bimetal oxide $CuFe_2O_4$ nanoparticles supported on mesoporous silica," *Journal of Materials Chemistry A*, vol.1, pp. 6742-6749, 2013.

[14] A. Manikandan, J. Judith Vijaya, L. John Kennedy and M. Bououdina, "Structural, optical and magnetic properties of $Zn_{1-x}Cu_xFe_2O_4$ nanoparticles prepared by microwave combustion method", *Journal of Molecular Structure*, vol. 1035, pp. 332–340, 2013.

[15] A. Manikandana, J. Judith Vijaya, M. Sundararajan, C. Meganathan, L. John Kennedy and M. Bououdina, "Optical and magnetic properties of Mg-doped $ZnFe_2O_4$ nanoparticles prepared by rapid microwave combustion method", *Superlattices and Microstructures*, vol.64, pp. 118-131, 2013.

[16] Nguyen Kim Thanh, To Thanh Loan, Luong Ngoc Anh, Nguyen Phuc Duong, Siriwat Soontaranon Nirawat Thammajak and Than Duc Hien, "Cation distribution in CuFe2O4 nanoparticles: Effects of Ni doping on magnetic properties," *Journal of Applied Physics*, vol. 120, p. 142115, 2016.

[17] Wang Zhang, Bo Quan, Chaedong Lee, Seung-Keun Park, Xinghe Li, Eunjin Choi, Guowang Diao and Yuanzhe Piao, "One-step facile solvothermal synthesis of copper ferrite-graphene composite as a high-performance supercapacitor material," *ACS Applied Materials and Interface*, vol. 7, pp. 2404-2414, 2015.

[18] S. Martinez-Vargas, A.I. Mtz-Enriquez, H. Flores-Zuñiga, A. Encinasc and J. Oliva, "Enhancing the capacitance and tailoring the discharge times of flexible graphene supercapacitors with cobalt ferrite nanoparticles," *Synthetic Metals*, vol. 264, p.116384, 2020.

[19] S. R. Jain, K. C. Adiga and V. R. Pai Verneker, "A New Approach to Thermochemical Calculations of Condensed Fuel-Oxidizer Mixtures," *Combustion and Flame*, vol. 40, No. 6, pp. 71-79, 1981.

[20] F. Daneshvar, A. Aziz, A.M. Abdelkader, T. Zhang, H. Sue, M.E.Welland,Porous SnO_2–Cu_xO nanocomposite thin film on carbon nanotubes as electrodes for high performance supercapacitors, *Nanotechnology*,vol. 30 pp. 015401–015410 2019.

[21] G. Theophil Anand , D. Renuka , R. Ramesh , L. Anandaraj , S. John Sundaram , G. Ramalingam , C. Maria Magdalane , A.K.H. Bashir , M. Maaza , K. Kaviyarasu, Green synthesis

of ZnO nanoparticle using prunus dulcis (Almond Gum) for antimicrobial and supercapacitor applications, *Surfaces and interfaces*, vol. 17, p. 100376, 2019.

[22] Salil U. Rege, Ralph T. Yang, "A novel FTIR method for studying mixed gas adsorption at low concentrations: H_2O and CO_2 on NaX zeolite and γ-alumina", *Chemical Engineering Science*, vol. 56, pp. 3781–3796, 2001.

[23] P.C. Rath, J. Patra, D. Saikia, M. Mishra, C.M. Tseng, J. Chang, H. Kao, Comparative study on the morphology-dependent performance of various CuO nanostructures as anode materials for sodium-ion batteries, ACS Sustain. Chem. Eng. vol. 6, pp. 10876–10885, 2018.

[24] Bablu Mordina, Rudra Kumar, Nagendra Singh Neeraj, Alok Kumar Srivastava, Dipak Kumar Setua and Ashutosh Sharma, "Binder free high performance hybrid supercapacitor device based on nickel ferrite nanoparticle," *Journal of Energy Storage*, vol. 31, p. 101677, 2020.

[25] Unchista Wongpratat, Pannawit Tipsawat, Jessada Khajonrit, Ekaphan Swatsitang and Santi Maensiri, "Effects of Nickel and Magnesium on electrochemical performances of partial substitution in spinel ferrite," *Journal of Alloys and Compounds*, vol. 831, p. 154718, 2020.

[26] V. Vignesh, K. Subramani, M. Sathish and R. Navamathavan, "Electrochemical investigation of manganese ferrites prepared via a facile synthesis route for supercapacitor applications," *Colloids and Surfaces A*, vol. 538, pp. 668–677, 2018.

[27] Ankur Soam, Rahul Kumar, Dhirendranath Thatoi and Mamraj Singh, "Electrochemical Performance and Working Voltage Optimization of Nickel Ferrite/Graphene Composite based Supercapacitor," Journal *of Inorganic and Organometallic Polymers and Material*, vol. 020, p. 01540, 2020.

[28] Bhamini Bhujun, Michelle T.T. Tan, Anandan S. Shanmugam, "Evaluation of aluminium doped spinel ferrite electrodes for supercapacitor," *Ceramics International*, vol. 42 pp. 6457–6466, 2016.

[29] Tapas Das and Bhawna Verma, "Synthesis of polymer composite based on polyaniline-acetylene black-copper ferrite for supercapacitor electrodes, Polymer, vol. 168, pp. 61-69, 2019.

[30] B. Jansi Rani, G. Ravi, R. Yuvakkumar, V. Ganesh, S. Ravichandran, M. Thambidurai, A.P. Rajalakshmi and A. Sakunthala, "Pure and cobalt-substituted zinc-ferrite magnetic ceramics for supercapacitor applications, *Applied Physics A*, vol. 124, p.511, 2018.

[31] S.K. Shinde, S.M. Mohite, A.A. Kadam, H.M. Yadav, G.S. Ghodake, K.Y. Rajpure, D.S. Lee and D.-Y. Kim, "Effect of deposition parameters on spray pyrolysis synthesized CuO nanoparticle thin films for higher supercapacitor performance", *Journal of Electroanalytical Chemistry*, vol. 850, p. 113433, 2019.

[32] M.Khairy M.G.EI-Shaarawy M.A Mousa, “Characterization and super-capacitive properties of nancrystalline copper ferrite prepared via green and chemical methods,” *Materials Science and Engineering*, vol. 263, p. 114812, 2021.

[33] Jia Song, Wenting Li, Jianjiao Xin, Wenbo Wang, Kun Song, Xiaoshuang Chen and Guangming Yin “The continuous porous PEDOT:PSS film improves wettability and flexibility of the rGO/CoFe2O4 paper electrodes for symmetric supercapacitors,” *Applied Surface Science*, vol. 568, p. 150915, 2021.

[34] Amir mohammad Khosravi Ghasemi, Mohasen Ghorbani, Mohammad Solei manilashkenari and Noushin Nasiri, “Facile synthesize of PANI/GO/$CuFe_2O_4$ nanocomposite material with synergistic effect for superb performance supercapacitor,” *Electrochimica Acta*, vol. 439, p. 141685, 2023.

[35]B. Carmel Jeeva Mary, J. Judith Vijaya, Radhika R. Nair, A Mustafa, P. Stephen Selvamani, B. Saravanakumar, M. Bououdina and L. John Kennedy, “Reduced Graphene Oxide-Tailored $CuFe_2O_4$ Nanoparticles as an electrode Material for High-Performance Supercapacitors,” *Journal of Nanomaterials*, 2022.

[36]M. Zhu, D. Meng, C. Wang, and G. Diao, “Facile fabrication of hierarchically porous $CuFe_2O_4$ nanospheres with enhanced capacitance property,” *ACS Applied Materials & Interfaces*, vol. 5, no. 13, pp. 6030–6037, 2013.